nature microbiology

ARTICLES

https://doi.org/10.1038/s41564-018-0267-7

Microbial nitrogen limitation in the mammalian large intestine

Aspen T. Reese[1,2], Fátima C. Pereira[3], Arno Schintlmeister[3,4], David Berry[3], Michael Wagner[3,4], Laura P. Hale[5], Anchi Wu[2], Sharon Jiang[2], Heather K. Durand[2], Xiyou Zhou[6], Richard T. Premont[6], Anna Mae Diehl[2,6], Thomas M. O'Connell[7], Susan C. Alberts[1,8,9], Tyler R. Kartzinel[10], Robert M. Pringle[11], Robert R. Dunn[12], Justin P. Wright[1] and Lawrence A. David[2,13]*

Resource limitation is a fundamental factor governing the composition and function of ecological communities. However, the role of resource supply in structuring the intestinal microbiome has not been established and represents a challenge for mammals that rely on microbial symbionts for digestion: too little supply might starve the microbiome while too much might starve the host. We present evidence that microbiota occupy a habitat that is limited in total nitrogen supply within the large intestines of 30 mammal species. Lowering dietary protein levels in mice reduced their faecal concentrations of bacteria. A gradient of stoichiometry along the length of the gut was consistent with the hypothesis that intestinal nitrogen limitation results from host absorption of dietary nutrients. Nitrogen availability is also likely to be shaped by host–microbe interactions: levels of host-secreted nitrogen were altered in germ-free mice and when bacterial loads were reduced via experimental antibiotic treatment. Single-cell spectrometry revealed that members of the phylum Bacteroidetes consumed nitrogen in the large intestine more readily than other commensal taxa did. Our findings support a model where nitrogen limitation arises from preferential host use of dietary nutrients. We speculate that this resource limitation could enable hosts to regulate microbial communities in the large intestine. Commensal microbiota may have adapted to nitrogen-limited settings, suggesting one reason why excess dietary protein has been associated with degraded gut-microbial ecosystems.

The mammalian large intestine (the colon) is considered an hospitable environment for microbes. Microbial communities in the mammalian large intestine are among the densest on the planet (for example, humans have been found to harbour ~10^{13} cells in total comprising hundreds of species)[1,2]. The mammalian large intestine is full of active microbial cells[3] that aid in host nutrient acquisition, waste processing, pathogen resistance and immune regulation[4–6]. Relative to elsewhere in the gut, the large intestine has a more neutral pH, larger volume and longer retention time, leading to a greater proliferation of microbes[7]. By contrast, the host's primary uptake of dietary proteins, fatty acids and simple carbohydrates occurs in the small intestine[8,9]. We hypothesized that concentrations of essential elements are diminished in the large intestine, especially relative to demand, and become increasingly limiting for growth and replication of microbial cells along the length of the gut.

Nitrogen is likely to be among the limiting nutrients for bacteria in the large intestine as it is for many organisms in diverse environments worldwide[10]. Animals are frequently nitrogen limited and have evolved many physiological strategies to capture sufficient nitrogen from food[6]. These include peptide transport systems[11], precise regulation of amino acid transporters[12] and even the cultivation of obligate symbionts that fix nitrogen gas[13,14]. Yet, aside from the small subset of microbial taxa that can increase nitrogen supply to their hosts through fixation, studies using germ-free mammals have demonstrated that intestinal microbes, collectively, are more often net consumers of nitrogen and increase the protein requirement of their hosts[15]. Additionally, bacterial cells often have even higher nitrogen requirements than do eukaryotic cells[16]. Bacteria may consequently compete with their animal hosts for nitrogen. However, hosts have the opportunity to access the nitrogen in their food before many of their associated microbes do. Hosts therefore may reduce resource supply to the large intestine and thus influence the composition and functioning of resident microbial assemblages.

If nitrogen is limiting for the bacteria in the large intestine, a mismatch should exist between the carbon-to-nitrogen (C/N) ratios of gut microbes and those of digesta or faeces. In particular, elevated C/N ratios in resources relative to consumers, a phenomenon known as stoichiometric limitation, indicates that large amounts of food must be processed to gain sufficient nitrogen for organismal maintenance and growth[16]. Excess digested carbon must be excreted to maintain stoichiometric balance, which in turn is expected to diminish growth efficiency[17–19]. Because the range of percent carbon content in organisms is generally narrow, the C/N ratio of digestible material is an indicator of overall nitrogen availability[16]. In addition, total nitrogen can be considered in an absolute sense, independent of carbon, such as in the Geometric Framework model[20].

[1]Department of Biology, Duke University, Durham, NC, USA. [2]Department of Molecular Genetics and Microbiology, Duke University, Durham, NC, USA. [3]Department of Microbiology and Ecosystem Science, Division of Microbial Ecology, Research Network Chemistry Meets Microbiology, University of Vienna, Vienna, Austria. [4]Large-Instrument Facility for Advanced Isotope Research, Research Network Chemistry Meets Microbiology, University of Vienna, Vienna, Austria. [5]Department of Pathology, Duke University Medical Center, Durham, NC, USA. [6]Department of Medicine, Duke University Medical Center, Durham, NC, USA. [7]Department of Otolaryngology – Head & Neck Surgery, Indiana University School of Medicine, Indianapolis, IN, USA. [8]Department of Evolutionary Anthropology, Duke University, Durham, NC, USA. [9]Institute of Primate Research, National Museums of Kenya, Nairobi, Kenya. [10]Department of Ecology and Evolutionary Biology, Brown University, Providence, RI, USA. [11]Department of Ecology and Evolutionary Biology, Princeton University, Princeton, NJ, USA. [12]Department of Applied Ecology, North Carolina State University, Raleigh, NC, USA. [13]Center for Genomic and Computational Biology, Duke University, Durham, NC, USA. *e-mail: lawrence.david@duke.edu

Long-term effects of reduced nitrogen diets have been shown to improve health outcomes in animal models when considered through the lens of the Geometric Framework[21,22]. This is hypothesized to be due to nitrogen limiting the use of carbohydrates and thus altering microbial composition[23]. Still, the relative importance of removal of nitrogen compared to increased carbon intake as well as the importance of microbial responses to these diets is not well-established. If the modulation of nitrogen levels in the gut results in changes in abundance of total microbes, nitrogen would be termed absolutely limiting for microbial growth (cellular replication) in the gut. Such a result would imply that total gut bacterial load is constrained by an overall lack of nitrogen rather than by an imbalance between nitrogen and other resources.

Faecal C/N ratios (22.91 ± 11.22) of all 30 mammal species tested were 36–1,000% higher than gut bacterial C/N ratios (Fig. 1a), suggesting a widespread signature across the mammals of limited total nitrogen supply for gut bacteria. We found C/N ratios to be low (4.07 ± 0.24) in bacterial strains isolated from the human gut and grown in vitro (Supplementary Table 1), which is similar to C/N ratios of non-host associated bacteria in both aquatic and terrestrial environments (4.67 ± 1.38)[24,25]. Faeces, of course, includes microbial cells, host cells, undigested food and other waste. We did not separate these components, but the relatively low C/N ratios of microbial cells and their high abundance in faecal material[26] implies that the non-microbial material in faeces has an even higher C/N ratio than the faeces as a whole. In the mammals sampled, faecal C/N ratios were similarly high for both wild (24.27 ± 12.38, $n = 20$) and domesticated or captive species (21.14 ± 9.26, $n = 10$; Supplementary Table 2). Values varied more than seven-fold among species, with approximately 300% greater C/N ratios in herbivores than carnivores (Fig. 1a).

In addition to the difference arising from broad diet type, we expected differences in nitrogen supply related to subtler variation within feeding guilds. Animals that eat plants with low C/N ratios, such as woody plants and forbs[27], should have intestines in which total nitrogen is less limiting than animals that feed primarily on grasses having comparatively high C/N ratios. Indeed, within a group of East African mammals, we found a significant positive correlation between grass consumption (as assessed using DNA metabarcoding[28]) and C/N ratio ($\rho = 0.42$, $P < 0.001$, Spearman correlation; Fig. 1b). Physiological features, including body length, intestine length and gut type (simple, hindgut fermenter or ruminant), were also associated with C/N ratios ($P = 0.002$, $P = 0.04$ and $P = 0.03$, respectively, analysis of covariance (ANCOVA); Fig. 1c). These associations may reflect the well-known ability of hindgut fermenters and larger animals to subsist on lower-quality (higher C/N ratio) food than ruminants[29] and smaller animals[30], respectively. Therefore total nitrogen can differ dramatically with fine-scale variation in dietary composition, with lowest nitrogen availability in species that consume diets rich in carbon relative to nitrogen. Additional variation may be introduced by other physiological idiosyncrasies, for example in snowshoe hare (and other Leporidae), which engage in coprophagy to allow a second round of digestion of their high C/N ratio diet[31].

Having observed evidence of stoichiometric limitation in the mammalian gut, we next tested if nitrogen was absolutely limiting for microbial growth (in other words, whether an overall lack of nitrogen constrains total gut bacterial load). Experimental modulation of total dietary nitrogen input (via protein concentration) in mice led to shifts in faecal gut bacterial load consistent with the absolute nitrogen-limitation hypothesis. We fed mice three isocaloric diets (Supplementary Table 6), which varied in their casein protein levels: low (6%), control (20%) and high (40%). Higher-protein diets decreased faecal C/N ratio ($P < 0.001$, Kruskal–Wallis test; Fig. 1d, Supplementary Fig. 1a), which was in turn associated with changes in microbial load: bacterial concentration was greater in high-protein (low C/N ratio) conditions and reduced in low-protein conditions ($P = 0.017$, Kruskal–Wallis test; Fig. 1e, Supplementary Fig. 1b). Differences in diet did not significantly affect host weight gain or loss ($P = 0.9$, Kruskal–Wallis test; Supplementary Fig. 1d), suggesting that changes in the microbiota did not simply reflect poor host condition. However, microbiota changes may also have been responses to mouse diet intake[23] or varying faecal transit time due to altered cellulose levels[32], neither of which were tracked.

We next examined the extent to which mammalian hosts might induce nitrogen limitation via selective nitrogen uptake and delivery. Because 80–90% of host absorption of dietary nitrogen takes place in the small intestine[9], we predicted a longitudinal gradient of total nitrogen along the length of the gut. We found that C/N ratios increased from the proximal small intestine to the large intestine in laboratory mice (Supplementary Fig. 2a), with the distal small intestine and the large intestine exhibiting significantly higher C/N ratios than the proximal small intestine ($P < 0.05$, Tukey's Honest Significant Difference test). This variation was independent of microbial load in gut contents ($P = 0.14$, Spearman correlation; Supplementary Fig. 2b). These results are consistent with a model in which colonic microbes could experience total nitrogen limitation as a consequence of upstream host absorption of dietary nutrients.

Although hosts may alter nitrogen availability through dietary absorption, we hypothesized that gut bacterial loads could also shape the nitrogen landscape. We therefore treated mice with a broad-spectrum antibiotic cocktail (ampicillin, vancomycin, metronidazole and neomycin[33]). Faecal C/N ratios increased significantly relative to untreated animals after two days ($P < 0.001$, linear mixed effects model likelihood test; Fig. 2a). This change may have been due to load reductions altering nitrogen available in bacterial cells or through gut bacterial metabolism and subsequent host absorption. However, we found evidence that this increase reflected, at least in part, changes in host provisioning of nitrogen. During antibiotic treatment, host delivery of ^{15}N from an injected isotopically labelled amino acid, threonine, into the gut decreased more than two-fold ($P = 0.001$, Mann–Whitney U-test; Fig. 2b). We observed that expression of murine *Muc2*, a mucus protein coding gene, was also significantly reduced ($P < 0.05$, Wilcoxon signed rank tests; Fig. 2c); moreover, mucus thickness (reflecting overall mucus quantity) in the proximal colon tended to be lower in treated mice ($P = 0.1$, Mann–Whitney U-test; Supplementary Fig. 3b), as has been seen elsewhere[34]. Consistent with the finding that bacterial load influences nitrogen levels, we observed that levels of delivered ^{15}N isotopically labelled threonine across the gut were lower in germ-free mice than in conventional mice ($P < 0.001$, mixed-design analysis of variance (ANOVA); Supplementary Fig. 5b). This finding agrees with previous work demonstrating that germ-free mice have a thinner colonic firm mucus layer[35,36] or thinner colonic mucus layers overall[37]. Together, our data support a model where host secretion of nitrogen is responsive to changes in microbial load.

To obtain insights into the sources of nitrogen available to the bacteria in the large intestine, we performed stable-isotope tracer experiments in mice using two complementary approaches. First, we tracked host allocation and microbial use of dietary nitrogen by feeding mice chow with typical protein levels in which all nitrogen was delivered via spirulina (*Arthrospira*) in the form of ^{15}N (the low natural abundance heavy isotope). While digestion of this diet may differ overall from standard mouse chow, as spirulina cells are not a typical component of mouse diet, consumption of it has not been found to negatively impact host health and this method ensured complete labelling of dietary nitrogen. Second, we considered the effect of host-secreted nitrogen by varying our source of labelled nitrogen in a separate cohort of mice, which received $^{15}N/^{13}C$ labelled threonine via tail-vein injection[38] as in the antibiotic and germ-free mouse experiments. This method represents a conservative estimate of host nitrogen secretion as it only includes

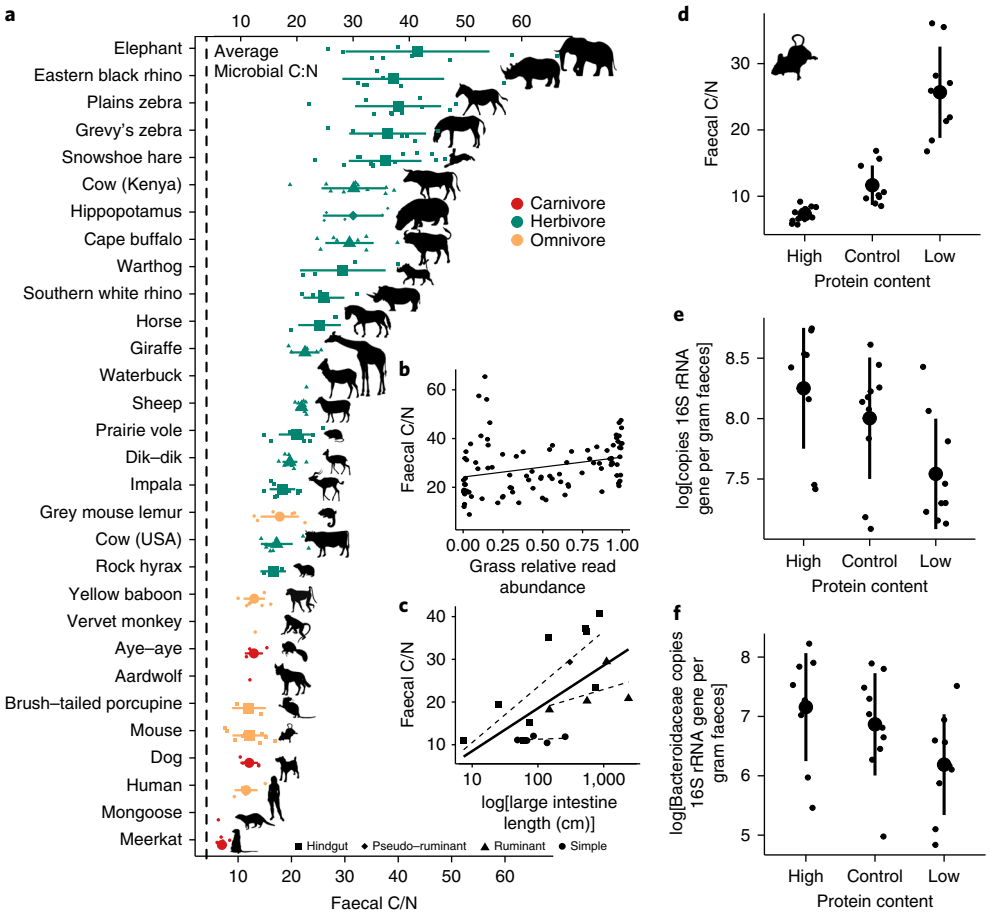

Fig. 1 | Mammalian faecal C/N ratio is linked to diet and physiology and controls microbial abundance in vivo. a–c, Faecal C/N ratio varied between mammals based on taxonomy, diet and physiology. Faecal C/N ratios from 30 mammal species ($n = 1$–15 individuals per species, mean = 7, see Supplementary Table 2) were higher than the average bacterial C/N ratios (4.07, vertical dashed line) from gut isolates grown in vitro ($n = 35$ strains, see Supplementary Table 1) and vary based on diet (colours) and gut physiology (shapes) (**a**). Faecal C/N ratios from East African herbivores and omnivores ($n = 16$ species, see Methods for list) were positively correlated (linear regression fit shown) with proportional representation of grasses in the diet based on DNA metabarcoding ($\rho = 0.42$, $P < 0.0001$, Spearman correlation; $n = 95$ faecal samples; gut physiology not shown; **b**). Mammalian faecal C/N ratio was also associated with the large intestine length (log transformed; $P = 0.04$, ANCOVA) and gut physiology ($P = 0.03$, ANCOVA; $n = 4$–9 species per physiological group (shapes), except pseudoruminant, which has $n = 1$; **c**). The solid line (**c**) shows linear regression fit for large intestine length overall, while dashed lines show linear regression fits for each gut architecture group. **d–f**, Altering dietary protein (Supplementary Table 5) for two weeks impacted murine gut nitrogen and microbiota. Murine faecal C/N ratio differed under altered-protein diets ($P = 5.87 \times 10^{-6}$, Kruskal–Wallis test; $n = 9$–10 mice per diet group; **d**). Microbial load, estimated by 16 S rRNA gene copy number via qPCR, also changed under altered-protein diets ($P = 0.017$, Kruskal–Wallis test; $n = 9$–10 mice per diet group; **e**). Bacteroidaceae abundance, calculated as 16 S ribosomal RNA gene copy number multiplied by their relative abundance, changed under altered-protein diets ($P = 0.05$, Kruskal–Wallis test; $n = 9$–10 mice per diet group; **f**). Large circles are means; bars show standard deviations. Animal icons courtesy of: J. A. Venter, H. H. T. Prins, D. A. Balfour and R. Slotow (vectorized by T. M. Keesey) (elephant, snowshoe hare, cape buffalo, warthog); DFoidl (modified by T. M. Keesey) (cow); M. Yrayzoz (vectorized by T. M. Keesey) (horse); Maky (vectorization), G. Skollar (photography) and R. Lewis (editing) (grey mouse lemur); Zimices (brush-tailed porcupine); D. Liao (mouse). All icons listed have been adapted under a Creative Commons license (https://creativecommons.org/licenses/by/3.0/) at phylopic.org.

labelled threonine; host-secreted compounds including non-threonine amino acids or amino sugars are found[39] but are not counted here. Taken together, these experiments revealed significant isotopic enrichment of gut tissue and gut contents from both secretions ($P < 0.05$, one-sample Wilcoxon tests; Fig. 3a and Supplementary Fig. 4a) and diet ($P < 0.05$, one-sample Wilcoxon tests; Fig. 3b and Supplementary Fig. 4a). The efficiency with which labelled nitrogen accumulated in large intestine gut contents (lumen and mucosa) did not differ significantly between the host-secreted and dietary delivery pathways ($P > 0.05$, Mann–Whitney U-tests; Fig. 3a,b). Our results fit with previous findings[23,38] and support an overall hypothesis that host amino acid secretions account for an appreciable fraction of the nitrogen available in the colon.

We next tested the hypothesis that nitrogen has distinct effects on different bacterial taxa in the gut. We used high-resolution secondary ion mass spectrometry (NanoSIMS) to measure uptake of both host-secreted and diet-sourced ^{15}N in the large intestine bacterial community with single-cell resolution. We confirmed that gut bacteria used nitrogen derived from both host diet and host secretions ($P < 0.001$, Kruskal–Wallis test; Supplementary Figs. 6 and 7). Combining NanoSIMS measurements with fluorescence in situ hybridization (FISH), we tested for nitrogen uptake by gut bacteria, including members of the Bacteroidales and *Clostridium* clusters XIVa/XIVb compared to other bacteria (see Supplementary Table 3 and 4, and Methods). Select Bacteroidales contribute to intestinal health and function[40], produce short-chain fatty acids for host

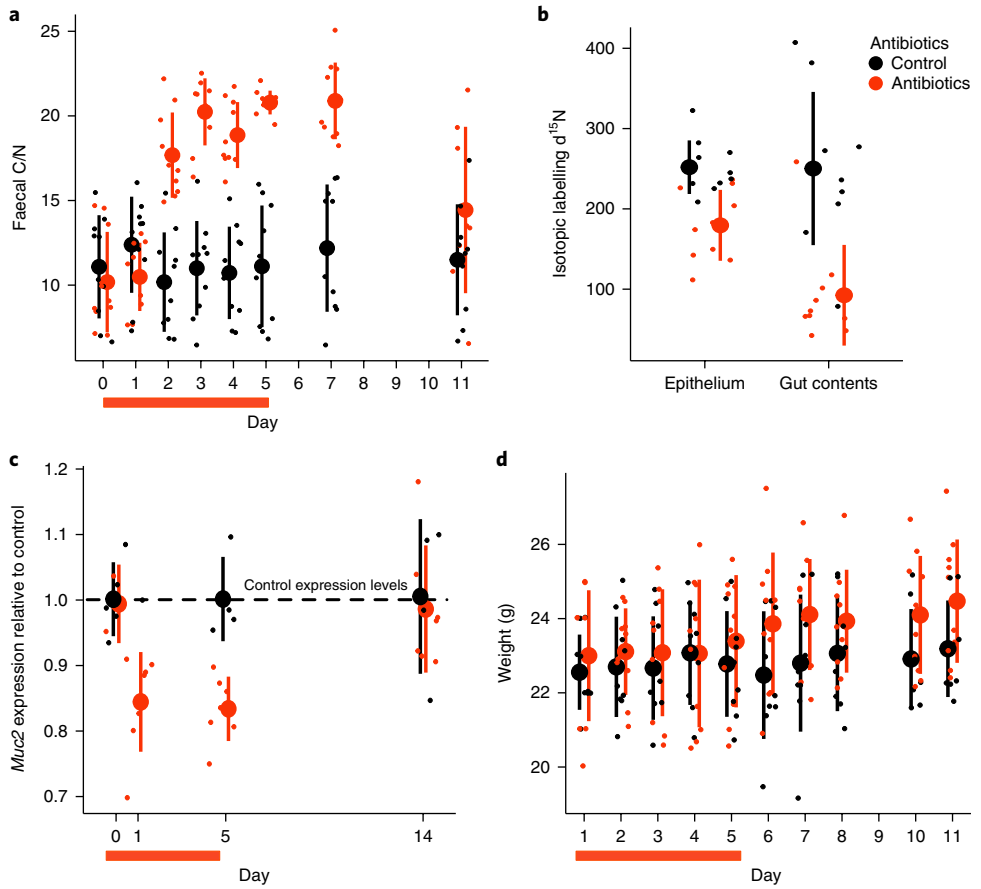

Fig. 2 | Antibiotics change gut nitrogen and host secretions. a, Antibiotic cocktail (ampicillin, vancomycin, metronidazole and neomycin) treatment induced a significant increase in faecal C/N ratio ($P = 2.647 \times 10^{-11}$, linear mixed effects model likelihood test; $n = 9$–10 mice per treatment group), followed by re-convergence within 6 days post-treatment. **b**,**c**, This increase is concomitant with decreases in nitrogen secretion as measured by isotopic label delivery to epithelial tissue and gut contents ($P = 0.001$, Mann–Whitney *U*-tests; $n = 10$ mice per treatment group) (**b**) and mucin production (measured as *Muc2* expression) relative to control levels (dotted line) during treatment ($P = 1.0$, 0.016, 0.016 and 0.58 Wilcoxon signed rank tests for treated mice relative to control average on days 0, 1, 5 and 14, respectively; $n = 6$ treated mice) (**c**). **d**, Mouse weight increased more over the 11 day experiment in antibiotic-treated mice than in control mice ($P = 0.0002$, linear mixed effects model likelihood test). Red bars under the *x* axis indicate the 5 day course of antibiotics. Large circles are means; bars show standard deviations.

uptake[41] and digest glycans into products on which other commensal microbiota can feed[42]. Consistent with previous observations[38], single-cell measurements in mice treated with $^{15}N/^{13}C$ labelled threonine injections showed that the Bacteroidales consumed host-secreted nitrogen more readily than the targeted Clostridia ($P < 0.05$, Bonferroni-corrected Mann–Whitney *U*-tests; Fig. 3c). These patterns are congruous with a model where members of the order Bacteroidales are initially sensitive, more so than typical gut microbiota species, and probably promoted by increases in host-secreted nitrogen. In support of this model, the abundance of Bacteroidales is known to be heightened in hibernating[43] and fasting[44] animals, where secretions are the primary source of all nutrients to the microbiota.

We also found evidence that members of the Bacteroidales were sensitive to dietary nitrogen. Single-cell measurements in mice treated with ^{15}N-labelled spirulina indicated that Bacteroidales were more likely to consume dietary nitrogen than other taxa measured ($P < 0.05$, Bonferroni-corrected Mann–Whitney *U*-tests; Fig. 3d). Notably, we observed in our dietary manipulation experiments that Bacteroidaceae (the most abundant family in the Bacteroidales in laboratory mice) increased with greater nitrogen supply ($P = 0.05$, Kruskal–Wallis test; Fig. 1f and Supplementary Fig. 1d). These findings contrast with a recent model suggesting that the Bacteroidetes should decrease with higher nitrogen intake[23]—a difference potentially due to that model's use of relative abundance data as compared to absolute bacterial abundances here. Their findings do, however, corroborate our observation that there is genus-level variation in response to greater dietary nitrogen supply, including increases in the Firmicutes family Lachnospiraceae (Supplementary Table 5). This observation may be explained by ecological phenomena such as cross-feeding or variation in nitrogen utilization strategies at finer taxonomic levels but will require further work to clarify.

Collectively, our findings suggest ecological and evolutionary mechanisms by which mammals and gut microbiota co-evolved[45]. By secreting nutrients into the large intestine or altering digestion, mammals could attenuate nitrogen limitation to upregulate preferred bacterial taxa such as members of the Bacteroidales (or to downregulate these same taxa by withholding secretions), thereby adjusting the aggregate digestive and metabolic functions of the gut-microbial community. This regulatory mechanism would entail a cost; a reduced need for nitrogen secretions may be one cause of antibiotic-associated weight gain, which is a phenomenon[46] observed in our mice ($P < 0.001$, linear mixed effects model likelihood test; Fig. 2d). Evolutionary theory predicts such a cost is worthwhile when animals interact with a diverse but beneficial

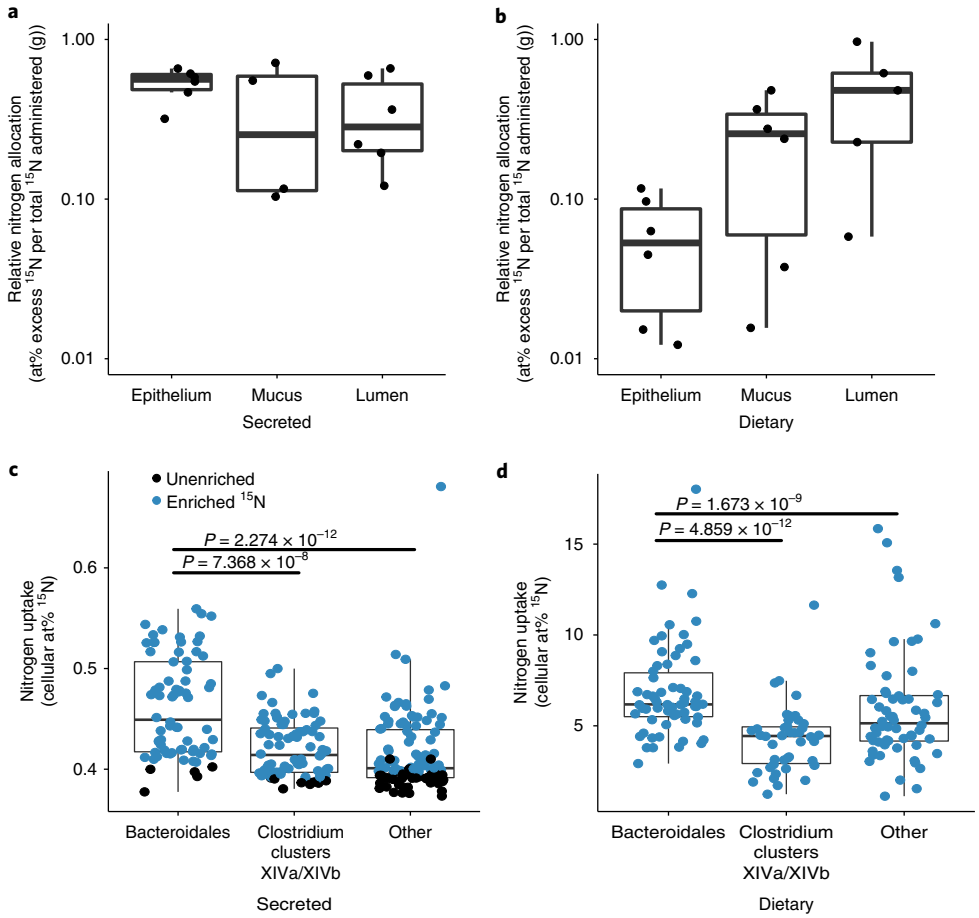

Fig. 3 | Microbes use nitrogen from host diet and secretions. a,**b**, Nitrogen in the gut is sourced both from host diet and host secretions. ^{15}N isotope enrichment (adjusted for total ^{15}N administered) was significantly different from zero for both injected threonine secretions (**a**) and dietary nitrogen (**b**) in large intestine epithelium, mucosa and lumen layers (null hypothesis: $\mu = 0$; $P = 0.03$, one-sample Wilcoxon tests; $n = 6$ mice per treatment). **c**,**d**, For large intestine gut microbiota from mice treated with labelled nitrogen, single-cell isotopic enrichment was quantified by NanoSIMS following FISH to distinguish between microbial taxonomic groups ($n = 2$ mice per treatment group). Bacteroidales were disproportionate nitrogen consumers relative to other bacterial taxa: cells targeted by the Bacteroidales probe (Bac303) were more highly enriched for ^{15}N from host-secreted labelled threonine ($n = 72$–110 cells per target; **c**) and also from host diet ($n = 42$–62 cells per target; **d**) than the *Clostridium* cluster XIVa and XIVb-specific (Erec482) or other DAPI-stained cells ($P < 0.05$, Bonferroni-corrected Mann–Whitney *U*-tests). Bars indicate groups that differed significantly from Bacteroidales. Isotope enrichment is reported as atom per cent (at%, the proportional representation of the heavy isotope multiplied by 100; **c** and **d**) or as atom per cent excess (the difference between atom per cent of the treated sample and the average control; **a** and **b**; see Methods). Blue points refer to cells significantly enriched in ^{15}N. Boxplots summarize all cells (enriched and unenriched) and show median and quartiles; whiskers show the 1.5×interquartile range.

microbiota, providing the host with a 'dial' to fine-tune gut-microbial communities in response to dietary, physiological and environmental variation[47]. Future work should elucidate the molecular and physiological mechanisms underpinning secretion dynamics, explore the magnitude of costs to the host and probe the conditions associated with changes in nitrogen supply to the gut within hosts over time and between host species. In particular, co-limitation with other nutrients[48], such as phosphorus, is likely in all animals. We predict carnivores with high nitrogen diets, short guts and low faecal C/N ratios may be especially likely to modulate co-limiting nutrient levels in order to regulate their microbiota.

Our model would also predict that competitive advantages for secretion-consuming bacteria might be eliminated (and mutualistic benefits reduced) if nitrogen supply to the large intestine exceeded some critical threshold. Indeed, when the human gut experiences nitrogen excess (for example with high-protein diet interventions), the microbiota quickly shift composition[49] and harmful metabolic products including ammonia, nitrosamines and sulfide are expected to accumulate[50]. High-protein diets are also associated with reductions in longevity in animals[22]. Thus, loss of microbial nitrogen limitation in the gut may resemble the environmental phenomenon of eutrophication in which excess nutrient delivery alters community composition and degrades ecosystem services[51].

Methods

Conventional mouse experiments. All mouse experiments were conducted in accordance with National Institute of Health Guide for the Care and Use of Laboratory Animals using protocols approved by the Duke University Institutional Animal Care & Use Committee. Male C57BL/6 mice (Charles River Laboratories) 8–10 weeks of age with a native microbiota were used for all manipulative experiments. Mice were kept in a conventional laboratory animal facility at Duke University and fed PMI Labdiet 5001 chow (20% protein; 12.5 ± 0.9 C/N ratio).

Animal faecal samples and gut-length estimates. Yellow baboon (*Papio cynocephalus*, $n = 8$, sex unspecified) faeces were collected from free-living baboons in the Amboseli basin of Kenya. Freshly dropped samples were collected within minutes when a known animal was observed defaecating. These samples were collected under protocols approved by the Duke University Institutional Animal Care & Use Committee. Each sample was homogenized and stored in 95% ethanol at a 2.5:1 ratio of ethanol to faeces for transportation to the University of Nairobi.

There the ethanol was allowed to evaporate and the samples were stored at −20 °C until freeze-drying at 30 mTorr to below −50 °C. Samples were then sifted and stored at −80 °C until processing for elemental analysis. Gut length was extracted from data on olive baboon (*Papio anubis*)[52].

Fresh faecal samples from Gunther's dik dik (*Madoqua guentheri*, $n=10$), impala (*Aepyceros melampus*, $n=10$), domestic Boran cattle (*Bos indicus*, $n=10$), cape buffalo (*Syncerus caffer*, $n=10$), plains zebra (*Equus quagga*, $n=10$), Grevy's zebra (*Equus grevyi*, $n=9$), African elephant (*Loxodonta africana*, $n=10$), white rhinoceros (*Ceratotherium simum*, $n=5$), vervet monkey (*Chlorocebus pygerythrus*, $n=1$), black rhinoceros (*Diceros bicornis*, $n=7$), reticulated giraffe (*Giraffa caemlopardalis reticulata*, $n=5$), hippopotamus (*Hippopotamus amphibious*, $n=5$), crested porcupine (*Hystrix cristata*, $n=2$), white-tailed mongoose (*Ichneumia albicauda*, $n=1$), waterbuck (*Kobus ellipsiprymnus*, $n=1$), warthog (*Phacochoerus africanus*, $n=6$), rock hyrax (*Procavia capensis*, $n=2$) and aardwolf (*Proteles cristata*, $n=1$) were collected at the Mpala Research Centre and Conservancy in central Kenya. These species, except for aardwolf and white-tailed mongoose, make up the East African herbivores and omnivores included in Fig. 1b,c. All individuals were adults but data on their sex was not uniformly available. All samples were collected under protocols approved by the Princeton University Institutional Animal Care & Use Committee. We obtained adult gut-length estimates from the literature[52–54] for a phylogenetically diverse subset of these species: aardwolf, vervet monkey, hyrax, dik dik, plains zebra, black rhinoceros, hippopotamus, giraffe, elephantand cattle, as well as for the brush-tailed porcupine *Atherurus africanus* (as a proxy *H. cristata*). We used only African *Bos indicus* data and not North American cattle (*Bos taurus*) for analysing C/N ratio relationships because the former were free-ranging.

Faecal samples from domestic sheep (*Ovis aries*, $n=10$), horse (*Equus ferus caballus*, $n=4$) and domestic cattle (*Bos taurus*, $n=10$) were obtained from adult animals on farms in New Jersey, USA. The sex of each individual was not available. Samples were collected non-invasively and were not subject to an animal care protocol. Gut length was identified for sheep[52] and horse[54].

Meerkat (*Suricata suricatta*, $n=9$) faecal samples were collected from a wild population in South Africa's Kalahari desert. Adults of both sexes were included. All samples were collected under protocols approved by the Duke University Institutional Animal Care & Use Committee.

Healthy human subjects ($n=5$), who reported no use of antibiotics in the month before enrolment, provided stool samples. Informed consent was obtained from all subjects and the protocol, approved by the Duke Health Institutional Review Board, complied with relevant ethical obligations. Subjects collected samples by placing disposable commode specimen containers (Fisher Scientific) under their toilet seats before bowel movements. Intact stool samples (~10 g) were briefly stored in personal −20 °C freezers before transport to the laboratory for long-term storage at −80 °C in sterile collection tubes. Human gut-length data were obtained from a published report[52].

Adult snowshoe hares (*Lepus americanus*, $n=15$), collected from wild populations in Washington and Montana, were kept in a photoperiod- and temperature-controlled research facility at the NCSU College of Veterinary Medicine. The sex of each individual was not recorded at the time of collection. All animals are kept under protocols approved by the North Carolina State University Institutional Animal Care & Use Committee. Samples were collected within 8 h of defaecation and frozen at −20 °C. Gut-length data were obtained for European rabbit (*Oryctolagus cuniculus*)[52].

Grey mouse lemur (*Microcebus murinus*, $n=8$) and aye-aye (*Daubentoia madagascariensis*, $n=4$) adults were housed in a breeding colony at the Duke Lemur Center. Faecal samples from mouse lemurs were collected fresh during regular technician handling in the non-torpor season then stored at −80 °C. Faecal samples from aye-ayes were collected after an individual was observed defaecating then stored at −80 °C. The sex of each individual was not recorded at collection. All animals are kept under protocols approved by the Duke University Institutional Animal Care & Use Committee.

Prairie vole (*Microtus ochrogaster*, $n=10$) adults (4–5 months old) were sampled from a breeding population housed at NCSU for genetic and behavioural studies. Voles of both sexes in either single or group housing had faeces collected fresh during normal technician handling. The sex of each individual was not recorded at collection. All animals are kept under protocols approved by the North Carolina State University Institutional Animal Care & Use Committee. Gut-length data were obtained for meadow vole (*Microtus pennsylvanicus*)[52].

Dog faecal samples (*Canis lupus familiaris*, $n=5$) were collected from a genetic model population of glycogen storage disease. Samples were collected fresh following feeding and then prepared immediately for analysis. All individuals were adults but data on their sex were not recorded at collection. All animals are kept under protocols approved by the Duke University Institutional Animal Care & Use Committee. Gut-length data were extracted from a previous report[54].

Wild-type mouse (*Mus musculus*) data were extracted from baseline, control animals ($n=10$) in the antibiotic experiments (see below). Gut-length data were extracted from the control animals in a published report[55].

To determine the impact of physiology on faecal C/N ratio of mammalian species, we performed an analysis of covariance (ANCOVA). Individual physiological data were not available, so species mean C/N ratio was calculated. Log large intestine length, gut physiology (simple, hindgut fermenter or ruminant[56]) and total body length were extracted from the literature and included as predictor variables as such: C/N ratio ~ $\log_{10}$(total body length) + $\log_{10}$(large intestine length) + gut physiology. Interaction terms were not found to be significant ($p>0.05$) and so were not included in the model. This test and all other statistical tests were carried out in R (R core team, ver. 3.3). All statistical tests performed were non-parametric except where a Shapiro–Wilks test indicated that data were normally distributed, in which case parametric tests were used.

Mouse whole-gut samples. We humanely killed untreated wild-type mice and immediately removed their complete gastrointestinal tract. For total gut content analyses ($n=10$), lumen contents and mucosa were scraped from the proximal small intestine, the distal small intestine, the caecum and the large intestine and immediately dried.

DNA from total gut samples was extracted using the MoBio PowerSoil extraction kit. To estimate total bacterial abundance, quantitative PCR (qPCR) was performed on faecal DNA using the following primers: forward, 5′-ACTCCTACGGGAGGCAGCAGT-3′, reverse, 5′-GTATTACCGCGGCTGCTGGCAC-3′ (ref.[57]). Quantitative PCR assays were run using SYBR FAST qPCR Master Mix (KAPA) on a 7900HT Fast Real-Time PCR System (Applied Biosystems). Cycle-threshold values were standardized against a dilution curve of known concentration and then adjusted for the weight of faecal matter extracted.

C/N ratio analyses. All samples were dried to constant weight at 72 °C in a vacuum oven and then ground and homogenized. Samples were packed into aluminium cups and processed on a Carlo Erba Elemental Analyzer with zero-blank auto-sampler except for Kenyan and New Jersey samples, which were analysed at the University of California Santa Cruz Stable Isotope Facility (Dumas combustion in a Carlo Erba 1108 Elemental Analyzer coupled to a ThermoFinnigan Delta Plus XP isotope ratio mass spectrometer) or the Duke Environmental Stable Isotope Laboratory (ThermoFinnigan MAT Delta Plus paired with a Carlo Erba Elemental Analyzer equipped with a zero-blank auto-sampler). Faecal C/N ratio measurements were conducted on whole faeces, which includes microbial cells, dietary material, host secretions and sloughed host cells.

Reconstructing wild mammal diets with DNA metabarcoding. Grass typically has a higher C/N ratio than woody plants and other herbs[27] and so a diet rich in grass is expected to generate higher faecal C/N ratios. Herbivore and omnivore dietary compositions were reconstructed using DNA metabarcoding[58] on DNA extracted from the same faecal samples used for elemental analysis (following methods described in Kartzinel et al.[28]). In short, DNA was extracted using the Zymo Xpedition Soil/Faecal Mini Kit and the composition of dietary plant DNA was quantified using targeted amplicon sequencing of the chloroplast *trn*L-P6 marker[58,59]. Thermocycling included denaturing at 95 °C for 10 min, followed by 35 cycles of 95 °C for 30 s, 55 °C for 30 s and 72 °C for 30 s and ending with a 2 min extension at 72 °C. Sequence demultiplexing, quality control and identification were performed with *obitools* and *ecoPCR* (see ref.[28] for detailed processing information). Grass consumption by each herbivore or omnivore was estimated using as the relative read abundance (RRA) of the grass family, *Poaceae* (in other words, the proportion of all *trn*L-P6 sequence reads that were identified as grasses relative to non-grasses). These data are strongly correlated with $\delta^{13}C$ enrichment ($P<0.001$, $\rho=0.88$, Spearman correlation), a well-established proxy for the consumption of C_4 grasses relative to C_3 plants (trees, shrubs and herbs) by herbivores in African savannas[28,60].

The present analysis supplements data available from Kartzinel et al.[28]. First, 4–5 additional faecal samples were collected from each of the 7 wild herbivores at the same study site in Kenya during October 2014 and these were analysed for C/N ratio and DNA. Second, an additional set of 1–7 samples from 11 new species were collected from this Kenya study system in July 2016; all were analysed for C/N ratio and 9 were analysed for DNA (excluding white-tailed mongoose and aardwolf, which are carnivores). Third, all new DNA metabarcode data were combined with raw data used in the analyses of Kartzinel et al.[28] and reanalysed in conjunction with improvements in the local plant DNA reference library used to identify *trn*L-P6 DNA sequences—now including 1,828 fertile plant vouchers (~442 species). For the subsets of samples included in both analyses estimates of grass RRA were strongly correlated ($R^2=0.99$). Altogether, we included estimates of grass abundance and C/N ratio for 125 mammals ($N=1$–10 per species, mean = 6) with both measurements taken from a single fresh faecal sample collected from each individual.

Gut isolate C/N ratios. Published average values of bacterial C/N ratio ratios (4.67 ± 1.38) include only measurements of bacteria isolated from ocean and soil environments[24,25]. We collected clonal population C/N ratio values for 35 strains of 26 species of gut bacteria (Supplementary Table 1). These species represent the five most abundant phyla in the mammalian gut[56].

Bacterial strains were isolated from a single human faecal donor or obtained from a commercial strain collection of gut isolates (ATCC; Supplementary Table 1). Human gut isolates were identified with almost complete 16 S rRNA gene Sanger

sequencing (using primers 27-f and 1492-r numbered according to *Escherichia coli* reference[61]). Samples were cultured anaerobically at 37 °C on blood agar plates and checked for growth at 24 and 48 h. These were then used to inoculate 5 ml of modified Gifu Anaerobic Broth (mGifu; Gifu Anaerobic Medium (HiMedia Laboratories), 2 ml l^{-1} hemin, 5 ml l^{-1} menadione)[62]. This medium has a C/N ratio of 3.77 ± 0.01. After 24 h of anaerobic incubation at 37 °C, these liquid cultures were used to inoculate sterile 250 ml bottles containing 150 ml of mGifu. After another 24 h of anaerobic incubation at 37 °C, A_{600} levels of the cultures were measured using an Eppendorf BioPhotometer. If the absorbance A_{600} levels did not exceed 1, cultures were re-incubated anaerobically for 24 h. Once the A_{600} levels exceeded 1, the bottle was removed from the incubator and centrifuged at 5,000–7,000 r.p.m. for at least 10 min in an ultracentrifuge. The resulting supernatant was decanted. The pelleted cells were dried at 72 °C for 48 h to a constant weight. The dried cells were then packaged and measured with a Carlo Erba Elemental Analyzer with zero-blank auto-sampler.

Dietary protein manipulation. *Mouse diets.* Conventional mice fed standard chow (LabDiet Picolab 5053 irradiated diet; 20% protein) were weighed and fresh faecal samples were collected before the initiation of the study. Mice were then randomly assigned a treatment and separated into cages, housing pairs that received the same treatment ($n = 10$ mice per treatment, $n = 5$ cages per treatment). The sample size was chosen following a power analysis to allow for regression coefficient of population (β) less than 0.1. Treatments consisted of isocaloric diets of varied casein protein levels: low (6%; Envigo TD.90016), control (20%; TD.91352) and high (40%; TD.90018). Mice were allowed to feed ad libitum on these diets for the rest of the experiment. Faecal samples and mouse weights were collected 1, 2, 7 and 14 days after initiation of the diet (see Supplementary Fig. 1d). All faecal samples were immediately frozen. These samples were then used for C/N ratio analysis and 16 S rRNA gene qPCR as above (see C/N ratio analyses and Mouse whole-gut samples, respectively).

Microbial amplicon sequencing. We performed 16 S rRNA gene amplicon sequencing on mouse faecal samples throughout the dietary intervention to determine compositional responses to changes in nitrogen input. We performed sequencing using custom barcoded primers[63] and published protocols[63–65]. DNA was extracted from frozen samples using the MoBio PowerSoil DNA extraction kit. Sequencing was conducted on an Illumina MiniSeq with paired end 150 base pair reads. The absolute abundance of the Bacteroidaceae was estimated by multiplying the total 16 S rRNA gene copy number for a sample by the relative abundance of Bacteroidaceae identified by amplicon sequencing.

Antibiotic treatment to alter microbial load. *In vivo nitrogen dynamics under antibiotics.* Baseline faecal samples were collected at least 24 h before the first dose and then mice were placed in individual housing with supplementary enrichment and continued on their standard diet (LabDiet Picolab 5053 irradiated diet; 20% protein). Mice were orally gavaged with either 0.25 ml autoclaved deionized water (control, $n = 10$) or 0.25 ml of an antibiotic cocktail (treated, $n = 10$) daily for five days then tracked for one week following the end of treatment. Mice were weighed daily. The mice were randomly assigned a group with an equal number of mice in each group and researchers collecting data were blinded to the groupings until after the final dose was administered. The sample size was chosen following a power analysis to allow for β less than 0.1.

The antibiotic cocktail consisted of ampicillin (Gold Biotechnology) 1 mg ml^{-1}, vancomycin (Alfa Aeser) 5 mg ml^{-1}, neomycin (EMD Millipore) 10 mg ml^{-1} and metronidazole (Alfa Aeser) 10 mg ml^{-1} (after Reikvam et al.[33]). Fresh antibiotic cocktails were prepared every day. Throughout the experiment freshly voided faecal samples were collected and stored at −80 °C for downstream analysis. Microbial load, as measured by 16 S rRNA gene qPCR, was significantly reduced within 24 h and remained low throughout treatment ($P < 0.05$, Bonferroni-corrected Mann–Whitney *U*-tests; Supplementary Fig. 3a). Faecal C/N ratio ratio was measured with an Elemental Analyzer as above (C/N ratio analyses).

We performed linear mixed effects analysis to determine the effects of antibiotics on C/N ratio, microbial load and mouse weight. As fixed effects, we entered antibiotic treatment and time with an interaction term into the model. We included mouse identity as a random effect. The *P* values were obtained by likelihood ratio tests comparing the full model against a model including only time and mouse identity and were performed with the ANOVA function in the lme4 package[66].

Isotopic labelling. For an additional cohort of mice, a stable-isotope tracer experiment was performed on the last day of antibiotic treatment using the above protocol. Four hours before euthanasia on the final day of treatment, mice were treated with 1.8 µmol 98 at% $^{15}N/^{13}C$ threonine in autoclaved deionized water via a 50 µl lateral tail-vein injection[38]. This treatment allowed nitrogen secretion into the gut to be conservatively estimated by measuring heavy label delivery. Immediately following euthanasia, the whole large intestine was removed and sectioned into equal thirds, longitudinally and the distal section was used for isotope measurements. Total gut contents (mucus and lumen) were scraped out and dried. Colon epithelial tissue was dried separately. Samples were homogenized and ground for δ ^{15}N quantification at the Duke Environmental Isotope Laboratory.

RNA isolation and RT–PCR. Host mucin production was quantified as *Muc2* expression (*Muc2* is the major murine intestinal mucin[67]) measured in faeces. Total RNA was isolated from faecal pellets stored in RNALater (Thermo Fisher) using the MoBio PowerMicrobiome RNA Isolation kit with an added phenol chloroform extraction step. Using cDNA Prep Reverse Transcription Master Mix (Fluidigm), ≤15 ng RNA was reverse transcribed following manufacturer's instructions. Target transcripts were preamplified for 18 cycles and then diluted 10 times. RT–PCR was performed using a BioMark (Fluidigm) on a 48 × 48 chip with Taqman Fast Advanced Master Mix (Thermo Fisher). Three ERCC RNA Spike-in Mix (Thermo Fisher) positive controls and a non-target negative control of nuclease-free water were also run on the chip. *Muc2* expression levels were normalized to mouse *Actb* (ΔCt) expression for each time point for each mouse and then compared to the average of control mice for that time point (ΔΔCt). Fold change (2^ΔΔCt) is presented in Fig. 2c.

Mucus thickness measurements. The proximal third of the large intestine from mice killed on the final day of antibiotic treatment was stored in a tissue cassette for mucus thickness measurements. Tissue samples were fixed in Carnoy's solution (ethanol6:acetic acid3:chloroform1, v/v/v) for 4 h before being moved to 70% ethanol solution. Paraffin sections were then prepared, sectioned transversely and stained with Alcian blue stain to highlight mucus. Mucus thickness was measured on a light microscope with 8–10 fields measured and averaged per sample. Thickness measurements were carried out in a blinded fashion and only in regions where the mucus layer was flanked on the luminal edge by intestinal contents. Records of how many measurements were made for each sample are provided in Supplementary Table 7.

^{15}N tracer experiments. *Mass balance studies.* Stable-isotope tracer experiments were performed to quantify nitrogen delivery from the host via dietary and secreted pathways. The dietary group ($n = 6$ per time point) received a 25 µl gavage of a dilute heavy-labelled mouse chow solution (0.01 g chow per 1 ml PBS) where the chow had all nitrogen sourced from spirulina cells (Cambridge Isotope Laboratories). This chow can be fed to rodents for extended periods of time without adverse health impacts[68,69] and is expected to provide a similar nitrogen content as conventional chow. The secretion group ($n = 6$ per time point) received 1.8 µmol $^{15}N/^{13}C$ threonine in autoclaved deionized water via a 50 µl lateral tail-vein injection[38]. The control group ($n = 6$) received a $^{14}N/^{12}C$ L-threonine (Sigma-Aldrich) injection. Six mice per experimental treatment group were euthanized at 4 h after treatment and another six mice were euthanized per experimental treatment group at 6 h after treatment. All six control mice were euthanized after 4 h. Mice were kept in single housing with enrichment and all faecal pellets were collected from the time of treatment through euthanasia. The mice were randomly assigned a group but researchers were not blinded to treatment during sample collection. The sample size was chosen following a power analysis to allow for β less than 0.1. The short time-span of the experiment was chosen to allow for appearance of dietary material in the gut while still minimizing the likelihood of re-secretion of diet-delivered ^{15}N by limiting the time for host processing of dietary material. Some ^{15}N made available to the host through the spirulina chow may have nonetheless appeared in the gut after uptake and then subsequent re-secretion. This phenomenon would only lessen differences between the two experimental groups; it would not result in overestimating the importance of secretions.

Immediately after euthanasia, the gut contents were dissected out. Lumen material and then mucosa material were scraped from the large intestine, caecum and small intestine of each mouse. Total material from each of these compartments and the epithelium were dried to a constant weight at 72 °C then weighed. These samples were then ground and homogenized to prepare as above for C/N ratio analysis and sent to the Duke Environmental Isotope Laboratory for isotope enrichment analysis. Overall C/N ratio was not affected by treatment ($P = 0.13$, Bonferroni-corrected Mann–Whitney *U*-tests; Supplementary Fig. 4c) but did vary between compartments and layers ($P < 0.001$, Kruskal–Wallis tests; Supplementary Fig. 4d,e).

Atom per cent excess ^{15}N was calculated for each sample. We also calculated atomic per cent excess ^{15}N as a function of total label administered to determine the relative nitrogen allocation to gut site or microbial cells. First, atom per cent ^{15}N was calculated wherein for an element *X*, with heavy isotope *H* and light isotope *L*: $at\%^{H} X = H/(H+L) \times 100$. Atom per cent excess was then calculated as the difference between the atom per cent of a treated sample and the average atom per cent of all control (unlabelled) samples. Atom per cent excess was then divided by the total ^{15}N label administered (atom per cent label multiplied by %N and weight) to correct for differences in total ^{15}N added by the dietary and injection routes. Patterns were not meaningfully different between the 4 and 6 h time points and so only large intestine, 4 h data is presented in the main text. All results can be found in Supplementary Fig. 4a.

Germ-free studies. The same protocol as above was followed for quantification of nitrogen allocation in germ-free mice with only minor deviations as outlined below. Fifteen male C57BL/6 mice over the age of eight weeks, derived and maintained in the Duke Gnotobiotic facility, were allocated into three treatment groups (control, dietary and secreted; $n = 5$ per group). Sample size was determined

by the availability of age- and sex-matched C57BL/6 mice. Mice received treatment as outlined in Mass balance studies above and were maintained in sterile containers with supplementary hydration under a fume hood for the 4 h study period. Faeces were collected and quantified per group for each hour following treatment. Mice were killed after 4 h and total guts were harvested and processed as above. Atom per cent excess was calculated for each gut section (small intestine, caecum and large intestine) and tissue type (mucus, lumen and epithelium). Mucus was the attached portion, generally of host derivation, whereas the lumen samplers were the loose contents that ultimately get integrated into faecal pellets. Epithelium was all host tissue. Germ-free versus conventional mouse isotope data were analysed with a mixed-design ANOVA in the 'ez' package in R. Mouse was the case identifier with gut layer (epithelium, mucus and lumen) and compartment (small intestine, caecum and large intestine) as predictor variables, which varied within cases. Germ-free status was included as a predictor variable, which varied between cases. Greenhouse–Geisser epsilon corrections were used for variables that did not pass Mauchly's tests for sphericity.

For analysis of faecal C/N ratio (Supplementary Fig. 5a), germ-free C57BL/6 mouse samples were collected in a sterile manner during regular technician handling from the National Gnotobiotic Rodent Research Center at University of North Carolina at Chapel Hill and from the Duke Gnotobiotic facility. Samples were stored temporarily at −20 °C before being moved to −80 °C for long-term storage.

Single-cell study tracers. To quantify microbial utilization of host and dietary nitrogen, we performed a slightly different stable-isotope tracer experiment than for the Mass balance studies above (Supplementary Fig. 7a). Mice were not fed overnight and then offered chow with all protein sourced from spirulina cells (Cambridge Isotope Laboratories) for 1 h before being returned to normal mouse chow for 4 h and killed. The dietary treatment group ($n = 10$) received 1 h of chow with ^{15}N-labelled spirulina and no other treatment. This setup allowed for greater label delivery than could be achieved via gavage of chow in solution as performed above. The secretion group ($n = 10$) were offered ^{14}N spirulina chow for 1 h before receiving 1.8 µmol ^{15}N/^{13}C threonine in autoclaved deionized water via a 50 µl lateral tail-vein injection[38]. The control group ($n = 10$) received ^{14}N chow and a ^{14}N/^{12}C L-threonine (Sigma-Aldrich) injection. The mice were randomly assigned a group but researchers were not blinded to treatment during sample collection. The sample size was chosen following a power analysis to allow for β less than 0.1.

Immediately after euthanasia, the gut contents were dissected out and all lumen and mucosal material was scraped from the large intestine and small intestine. Samples were homogenized for each compartment for each mouse. Of these gut contents, two-thirds were immediately frozen for downstream sequencing and elemental analysis; one-third were fixed in 2% paraformaldehyde overnight at 4 °C and then washed in PBS before being stored at −20 °C in 60% ethanol/40% PBS until preparation for FISH.

Bulk analyses. We prepared 16 S rRNA gene amplicons as above but the sequencing was performed on an Illumina MiSeq with 250 paired end reads and the V2 kit at the Duke Molecular Physiology Institute. The experimental procedures did not result in significant differences in microbial community composition ($P > 0.05$, Permutational ANOVA (PERMANOVA) computed with 'adonis' function in the 'vegan' package; Supplementary Fig. 7d). We observed differences between the large intestine and small intestine composition across all treatment groups ($R^2 = 0.60$ $P = 0.001$, PERMANOVA).

Samples were prepared as above for C/N ratio analysis and sent to the Cornell Isotope Laboratory for isotope enrichment analysis on a ThermoFinnigan MAT Delta Plus paired with a Carlo Erba NC2500 Elemental Analyzer equipped with a low blank AS200 auto-sampler. Overall, both treatments produced significant bulk enrichment relative to ^{14}N controls ($P < 0.001$, Kruskal–Wallis test; Supplementary Fig. 7c) as well as significant cellular enrichment ($P < 0.001$, Kruskal–Wallis test; Supplementary Fig. 7b), indicating that they could be used to track microbial uptake. Similar to the compositional patterns, bulk C/N ratio measurements were not affected by treatment ($P = 0.09$, Kruskal–Wallis test) but did vary between compartments ($P = 0.02$, Mann–Whitney *U*-test; Supplementary Fig. 7e).

Single-cell analyses. Duplicate samples, randomly selected from each treatment group, were chosen for single-cell analysis. Flushed gut contents fixed with 4% formaldehyde stored in a 60% ethanol/40% PBS solution were used for FISH and NanoSIMS imaging. FISH was performed with fluorescently-labelled rRNA-targeted oligonucleotide probes[38] Bac303 (S-*-Bacto-0303-a-A-17-Cy3, 5′-CCA ATG TGG GGG ACC TT -3′) and Erec482 (S-*-Erec-0482-a-A-179-Cy5; GCT TCT TAG TCA RGT ACC G) (see Supplementary Table 3[70,71]) using a standard protocol[72]. To evaluate potential non-specific FISH probe binding, parallel samples were hybridized with the reverse complement of the bacterial probe EUB338 for all used dyes (NONEUB-5′-ACTCCTACGGGAGGCAGC-3′; ref. [38]). Samples were subsequently stained with DAPI (1 µg ml^{-1}; Sigma-Aldrich) for 5 min. Hybridized, DAPI-stained samples were imaged and marked on an epifluorescence laser microdissection microscope (LMD, Leica LMD 7000) as previously described[38].

NanoSIMS measurements were performed on an NS50L (Cameca) at the University of Vienna, Austria. Data were recorded as multilayer image stacks obtained by sequential scanning of a finely focused Cs^+ primary ion beam (about 80 nm spot size with 2 pA beam current) and detection of negative secondary ions and secondary electrons. Recorded images had a 512 × 512 pixel resolution and a field-of-view ranging from 47 × 47 to 72 × 72 µm^2. The mass spectrometer was tuned to achieve a mass resolving power (MRP) of >10.000 (according to Cameca's definition) for detection of C_2^- and CN^- secondary ions. Before data acquisition, which was performed as long-runs for sampling of entire cells, analysis areas were gently pre-sputtered by application of a Cs^+ dose density in the range from 2.3×10^{15} to 7.0×10^{15} ions cm^2. All images were recorded with a dwell time of 5–10 ms per pixel per cycle and accumulation of 23 to 30 cycles per image.

NanoSIMS images were processed using the WinImage software package (Cameca). Cells were identified in drift-corrected, stack-accumulated NanoSIMS images and manually verified with aligned FISH images (see Supplementary Fig. 6 for representative images). Cells that overlapped or were otherwise indistinguishable were not measured. Signal intensities were corrected for detector dead time on a per-pixel basis and quasi-simultaneous arrival (QSA) of C_2^- and CN^- secondary ions on a per-ROI basis. The QSA correction was performed according to the formalism suggested by previous work[73], applying sensitivity factors of 1.06 and 1.05 for C_2^- and CN^- ions, respectively (experimentally determined on dried yeast cells). $^{15}N/(^{14}N + ^{15}N)$ isotope fractions, designated as at% ^{15}N throughout the text, were calculated from $^{15}N/(^{14}N + ^{15}N) = {}^{12}C^{15}N^-/({}^{12}C^{14}N^- + {}^{12}C^{15}N^-)$. Summary statistics from each region of interest were calculated for single-cell analysis. A single field-of-view was collected for each treatment with technical replicates of 91–162 cells per field-of- view. Individual cells were considered significantly enriched in ^{15}N if the mean cellular at% ^{15}N was greater than five standard deviations above the mean at% ^{15}N of the unlabelled control cells and if the measurement error (5σ, Poisson) was smaller than the difference between the at% of the labelled cell and the mean at% of unlabelled control cells. The Poisson error (random measurement error due to counting statistics) was calculated by

$$\sigma_{POIS} = \frac{n}{(nL^- + H^-)}\sqrt{(L^-)^2H^- + (L^-)^2H^-}$$

where L^- and H^- refer to the signal intensity (in counts) associated with the light and heavy isotope, respectively, and $n = 1$ for detection of CN^- and $n = 2$ for detection of C_2^- secondary ions. Significant enrichment of cells relative to controls was documented from both labelling delivery paths ($P < 0.05$, Mann–Whitney *U*-tests; Supplementary Fig. 7b).

Reporting Summary. Further information on experimental design is available in the Nature Research Reporting Summary linked to this article.

Data availability

The 16S rRNA gene nucleotide sequences generated in this study can be downloaded from the European Nucleotide Archive under study accession numbers PRJEB26478 (protein manipulation and NanoSIMS experiments) and PRJEB26446 (antibiotics experiment). NanoSIMS and bulk isotopic data for the dietary and injected ^{15}N study is included in Supplementary Table 4. Other data that support these findings are available from the corresponding author upon request.

Received: 1 May 2018; Accepted: 10 September 2018;
Published online: 29 October 2018

References

1. McFall-Ngai, M. Adaptive immunity: care for the community. *Nature* **1145**, 153 (2007).
2. Sender, R., Fuchs, S. & Milo, R. Are we really vastly outnumbered? Revisiting the ratio of bacterial to host cells in humans. *Cell* **164**, 337–340 (2016).
3. Lennon, J. T. & Jones, S. E. Microbial seed banks: the ecological and evolutionary implications of dormancy. *Nat. Rev. Microbiol.* **9**, 119–130 (2011).
4. Hooper, L. V. & Macpherson, A. J. Immune adaptations that maintain homeostasis with the intestinal microbiota. *Nat. Rev. Immunol.* **10**, 159–169, https://doi.org/10.1038/nri2710 (2010).
5. Backhed, F., Ley, R. E., Sonnenburg, J. L., Peterson, D. A. & Gordon, J. I. Host–bacterial mutualism in the human intestine. *Science* **307**, 1915–1920 (2005).
6. Fuller, M. F. & Reeds, P. J. Nitrogen cycling in the gut. *Annu. Rev. Nutr.* **18**, 385–411 (1998).
7. Walter, J. & Ley, R. The human gut microbiome: ecology and recent evolutionary changes. *Annu. Rev. Microbiol.* **65**, 411–429 (2011).
8. Carmody, R. N. & Turnbaugh, P. J. Gut microbes make for fattier fish. *Cell Host Microbe* **12**, 259–261 (2012).
9. Borgstrom, B., Dahlqvist, A., Lundh, G. & Sjovall, J. Studies of intestinal digestion and absorption in the human. *J. Clin. Invest.* **36**, 1521–1536 (1957).
10. Elser, J. J. et al. Global analysis of nitrogen and phosphorus limitation of primary producers in freshwater, marine and terrestrial ecosystems. *Ecol. Lett.* **10**, 1135–1142 (2007).

11. Gardner, M. L. G. Gastrointestinal absorption of intact proteins. *Annu. Rev. Nutr.* **8**, 329–350 (1988).
12. Ferraris, R. P. & Carey, H. V. Intestinal transport during fasting and malnutrition. *Annu. Rev. Nutr.* **20**, 195–219 (2000).
13. Lilburn, T. G. et al. Nitrogen fixation by symbiotic and free-living spirochetes. *Science* **292**, 2495–2498 (2001).
14. Vecherskii, M. V., Naumova, E. I., Kostina, N. V. & Umarov, M. M. Some specific features of nitrogen fixation in the digestive tract of the European beaver (Castor fiber). *Dokl. Biol. Sci.* **411**, 452–454 (2006).
15. Wostman, B. S. The germ-free animal in nutritional studies. *Annu. Rev. Nutr.* **1**, 257–279 (1981).
16. Sterner, R. W. & Elser, J. J. *Ecological Stoichiometry: The Biology of Elements from Molecules to the Biosphere* (Princeton Univ. Press, Princeton, 2002).
17. Frost, P. C. & Elser, J. J. Growth response of littoral mayflies to the phosphorus content of their food. *Ecol. Lett.* **5**, 232–240 (2002).
18. Elser, J. J. et al. Growth rate–stoichiometry couplings in diverse biota. *Ecol. Lett.* **6**, 936–943 (2003).
19. Fink, P. & Von Elert, E. Physiological responses to stoichiometric constraints: nutrient limitation and compensatory feeding in a freshwater snail. *Oikos* **115**, 484–494 (2006).
20. Simpson, S. J. & Raubenheimer, D. *The Nature of Nutrition: A Unifying Framework from Animal Adaptation to Human Obesity* (Princeton Univ. Press, Princeton, 2012).
21. Le Couteur, D. et al. The influence of macronutrients on splanchnic and hepatic lymphocytes in aging mice. *J. Gerontol. A Biol.* **70**, 1499–1507 (2014).
22. Solon-Biet, S. M. et al. Macronutrient balance, reproductive function and lifespan in aging mice. *Proc. Natl Acad. Sci. USA* **112**, 3481–3486 (2015).
23. Holmes, A. J. et al. Diet-microbiome interactions in health are controlled by intestinal nitrogen source constraints. *Cell Metab.* **25**, 140–151 (2017).
24. Zimmerman, A. E., Allison, S. D. & Martiny, A. C. Phylogenetic constraints on elemental stoichiometry and resource allocation in heterotrophic marine bacteria. *Environ. Microbiol.* **16**, 1398–1410 (2013).
25. Mouginot, C. et al. Elemental stoichiometry of Fungi and Bacteria strains from grassland leaf litter. *Soil Biol. Biochem.* **76**, 278–285 (2014).
26. Stephen, A. M. & Cummings, J. H. The microbial contribution to human faecal mass. *J. Med. Microbiol.* **13**, 45–56 (1980).
27. Tjoelker, M. G., Craine, J. M., Wedin, D., Reich, P. B. & Tilman, D. Linking leaf and root trait syndromes among 39 grassland and savannah species. *New Phytol.* **167**, 493–508 (2005).
28. Kartzinel, T. R. et al. DNA metabarcoding illuminates dietary niche partitioning by African large herbivores. *Proc. Natl Acad. Sci. USA* **112**, 8019–8024 (2015).
29. Kleynhans, E. J., Jolles, A. E., Bos, M. & Olff, H. Resource partitioning along multiple niche dimensions in differently sized African savanna grazers. *Oikos* **120**, 591–600 (2011).
30. Müller, D. W. H. et al. Assessing the Jarman–Bell Principle: scaling of intake, digestibility, retention time andgut fill with body mass in mammalian herbivores. *Comp. Biochem. Phys. A* **164**, 129–140 (2013).
31. Hirakawa, H. Coprophagy in leporids and other mammalian herbivores. *Mamm. Rev.* **31**, 61–80 (2001).
32. Kashyap, P. C. et al. Complex interactions among diet, gastrointestinal transit, and gut microbiota in humanized mice. *Gastroenterology* **144**, 967–977 (2013).
33. Reikvam, D. H. et al. Depletion of murine intestinal microbiota: effects on gut mucosa and epithelial gene expression. *PLoS ONE* **6**, e17996 (2011).
34. Wlodarska, M. et al. Antibiotic treatment alters the colonic mucus layer and predisposes the host to exacerbated Citrobacter rodentium-induced colitis. *Infect. Immun.* **79**, 1536–1545 (2011).
35. Johansson, M. E. et al. The inner of the two Muc2 mucin-dependent mucus layers in colon is devoid of bacteria. *Proc. Natl Acad. Sci. USA* **105**, 15064–15069 (2008).
36. Johansson, M. E. et al. Normalization of host intestinal mucus layers requires long-term microbial colonization. *Cell Host. Microbe* **18**, 582–592 (2015).
37. Li, H. et al. The outer mucus layer hosts a distinct intestinal microbial niche. *Nat. Commun.* **6**, 3292 (2015).
38. Berry, D. et al. Host-compound foraging by intestinal microbiota revealed by single-cell stable isotope probing. *Proc. Natl Acad. Sci USA* **110**, 4720–4725 (2013).
39. Tailford, L. E., Crost, E. H., Kavanaugh, D. & Juge, N. Mucin glycan foraging in the human gut microbiome. *Front. Genet.* **6**, 81 (2015).
40. Ley, R. E., Lozupone, C. A., Hamady, M., Knight, R. & Gordon, J. I. Worlds within worlds: evolution of the vertebrate gut microbiota. *Nat. Rev. Microbiol.* **6**, 776–788 (2008).
41. den Besten, G. et al. The role of short-chain fatty acids in the interplay between diet, gut microbiotaand host energy metabolism. *J. Lipid Res.* **54**, 2325–2340 (2013).
42. Koropatkin, N. M., Cameron, E. A. & Martens, E. C. How glycan metabolism shapes the human gut microbiota. *Nat. Rev. Microbiol.* **10**, 323–335 (2012).
43. Carey, H. V., Walters, W. A. & Knight, R. Seasonal restructuring of the ground squirrel gut microbiota over the annual hibernation cycle. *Am. J. Physiol. Regul. Integ. Comp. Physiol.* **304**, R33–R42 (2013).
44. Costello, E. K., Gordon, J. I., Secor, S. M. & Knight, R. Postprandial remodeling of the gut microbiota in Burmese pythons. *ISME J.* **4**, 1375–1385 (2010).
45. McFall-Ngai, M. et al. Animals in a bacterial world, a new imperative for the life sciences. *Proc. Natl Acad. Sci. USA* **110**, 3229–3236 (2013).
46. Cho, I. et al. Antibiotics in early life alter the murine colonic microbiome and adiposity. *Nature* **488**, 621–626 (2012).
47. Foster, K. R., Schluter, J., Coyte, K. Z. & Rakoff-Nahoum, S. The evolution of the host microbiome as an ecosystem on a leash. *Nature* **548**, 43–51 (2017).
48. Kaspari, M. & Powers, J. S. Biogeochemistry and geographical ecology: embracing all twenty-five elements required to build organisms. *Am. Nat.* **188**, S62–S73 (2016).
49. David, L. A. et al. Diet rapidly and reproducibly alters the human gut microbiome. *Nature* **505**, 559–563 (2014).
50. Scott, K. P., Gratz, S. W., Sheridan, P. O., Flint, H. J. & Duncan, S. H. The influence of diet on the gut microbiota. *Pharmacol. Res.* **69**, 52–60 (2013).
51. Smith, V. H., Tilman, G. D. & Nekola, J. C. Eutrophication: impacts of excess nutrient inputs on freshwater, marine and terrestrial ecosystems. *Environ. Pollut.* **100**, 179–196 (1999).
52. Stevens, C. E. & Hume, I. D. *Comparative Physiology of the Vertebrate Digestive System* 2nd edn (Cambridge Univ. Press, Cambridge, 1995).
53. Pérez, W., Lima, M. & Clauss, M. Gross anatomicy of the intestine in the giraffe (*Giraffa camelopardalis*). *Anat. Histol. Embryol.* **38**, 432–435 (2009).
54. Kararli, T. T. Comparison of the gastrointestinal anatomicy, physiology and biochemistry of humans and commonly used laboratory animals. *Biopharm. Drug Dispos.* **16**, 351–380 (1995).
55. Aust, G. et al. Mice overexpressing CD97 in intestinal epithelial cells provide a unique model for mammalian postnatal intestinal cylindrical growth. *MBoC* **24**, 2256–2268 (2013).
56. Ley, R. E. et al. Evolution of mammals and their gut microbes. *Science* **320**, 1647–1651 (2008).
57. Bergström, A. et al. Introducing GUt Low-Density Array (GULDA) – a validated approach for qPCR-based intestinal microbial community analysis. *FEMS Microbiol. Lett.* **337**, 38–47 (2012).
58. Taberlet, P. et al. Power and limitations of the chloroplast trnL (UAA) intron for plant DNA barcoding. *Nucleic Acids Res.* **3**, e14 (2007).
59. De Barba, M. et al. DNA metabarcoding multiplexing and validation of data accuracy for diet assessment: application to omnivorous diet. *Mol. Ecol. Resour.* **14**, 306–323 (2014).
60. Cerling, T. E., Harris, J. M. & Passey, B. H. Diets of East African Bovidae based on stable isotope analysis. *J. Mammal.* **84**, 456–470 (2003).
61. Frank, J. A. et al. Critical evaluation of two primers commonly used for amplification of bacterial 16S rRNA genes. *Appl. Environ. Microb.* **74**, 2461–2470 (2008).
62. Rettedal, E. A., Gumpert, H. & Sommer, M. O. Cultivation-based multiplex phenotyping of human gut microbiota allows targeted recovery of previously uncultured bacteria. *Nat. Commun.* **5**, 4714 (2014).
63. Caporaso, J. G. et al. Global patterns of 16S rRNA diversity at a depth of millions of sequences per sample. *Proc. Natl Acad. Sci. USA* **108**, 4516–4522 (2011).
64. Caporaso, J. G. et al. Ultra-high-throughput microbial community analysis on the Illumina HiSeq and MiSeq platforms. *ISME J.* **6**, 1621–1624 (2012).
65. Maurice, C. F., Haiser, H. J. & Turnbaugh, P. J. Xenobiotics shape the physiology and gene expression of the active human gut microbiome. *Cell* **152**, 39–50 (2013).
66. Bates, D., Maechler, M., Bolker, B. & Walker, S. Fitting linear mixed-effects models using lme4. *J. Stat. Softw.* **67**, 1–48 (2015).
67. Park, S. W. et al. The protein disulphide isomerase AGR2 is essential for production of intestinal mucus. *Proc. Natl Acad. Sci. USA* **106**, 6950–6955 (2009).
68. McClatchy, D. B., Dong, M.-Q., Wu, C. C., Venable, J. D. & Yates, J. R. III 15N metabolic labelling of mammalian tissue with slow protein turnover. *J.Proteome Res.* **6**, 2005–2010 (2007).
69. McClatchy, D. B., Liao, L., Park, S. K., Venable, J. D. & Yates, J. R. III Quantification of the synaptosomal proteome of the rat cerebellum during post-natal development. *Genome Res.* **17**, 1378–1388 (2007).
70. Franks, A. H. et al. Variations of bacterial populations in human faeces measured by fluorescent in situ hybridization with group-specific 16S rRNA-targeted oligonucleotide probes. *Appl. Environ. Microbiol.* **64**, 3336–3345 (1998).
71. Manz, W., Amann, R., Ludwig, W., Vancanneyt, M. & Schleifer, K. H. Application of a suite of 16S rRNA-specific oligonucleotide probes designed to investigate bacteria of the phylum Cytophaga–Flavobacter–Bacteroides in the natural environment. *Microbiology* **142**, 1097–1106 (1996).
72. Daims, H., Stoecker, K. & Wagner, M. in *Molecular Microbial Ecology* (eds Osborn, M. & Smith, C) Ch. 9 (Taylor & Francis, London, 2004).

73. Slodzian, G., Hillion, F., Stadermann, F. J. & Zinner, E. QSA influences on isotopic ratio measurements. *Appl. Surf. Sci.* **231**, 874–877 (2004).

Acknowledgements

W. Cook carried out C/N ratio measurements in the Duke Environmental Isotope Laboratory. Samples were provided by S. Mills and D. Lafferty (snowshoe hare); E. Ehmke (lemurs); L. McGraw, A. Vogel and C. Clement (prairie vole); D. Koeberl, V. Sakach and L. Morgan (dog); C. Drea (meerkat). Statistical advice was provided by K. Choudhury and S. Mukherjee. The manuscript was improved thanks to comments from J. Heffernan, J. Rawls and P. Turnbaugh. This work was funded by an NSF Doctoral Dissertation Improvement grant to A.T.R., J.P.W. and L.A.D. (grant no. DEB-1501495) and grants from the Hartwell Foundation, Alfred P. Sloan Foundation and Searle Scholars Programme to L.A.D. A.T.R. was supported by the NSF Graduate Research Fellowship Programme under grant no. DGE 1106401. F.C.P. was supported by a European Research Council Marie Curie Individual Fellowship (grant no. 658718). D.B. was supported in part by Austrian Science Fund (grant nos. P26127-B20 and P27831-B28) and European Research Council (Starting Grant: FunKeyGut 741623). M.W. was supported by the European Research Council via the Advanced Grant project 'NITRICARE 294343'. The contents of this paper are the responsibility of the authors and do not necessarily represent the views of the funding institutions.

Author contributions

A.T.R., F.P., A.S., D.B. and M.W. carried out FISH / NanoSIMS work. A.T.R., X.Z. and R.P. performed diet manipulation experiments. L.P.H., S.J. and H.K.D. processed samples. T.M.O., S.C.A., T.R.K. and R.M.P. contributed data. A.T.R. performed all other experiments. A.M.D., R.R.D. and J.P.W. were involved in study design. A.T.R. and L.A.D. designed the study, analysed data and wrote the paper. All authors discussed the results and commented on the manuscript.

Competing interests

The authors declare no competing interests.

Additional information

Supplementary is available for this paper at https://doi.org/10.1038/s41564-018-0267-7.

Reprints and permissions information is available at www.nature.com/reprints.

Correspondence and requests for materials should be addressed to L.A.D.

Publisher's note: Springer Nature remains neutral with regard to jurisdictional claims in published maps and institutional affiliations.

nature research

Corresponding author(s): Lawrence A. David

☐ Initial submission ☒ Revised version ☐ Final submission

Life Sciences Reporting Summary

Nature Research wishes to improve the reproducibility of the work that we publish. This form is intended for publication with all accepted life science papers and provides structure for consistency and transparency in reporting. Every life science submission will use this form; some list items might not apply to an individual manuscript, but all fields must be completed for clarity.

For further information on the points included in this form, see Reporting Life Sciences Research. For further information on Nature Research policies, including our data availability policy, see Authors & Referees and the Editorial Policy Checklist.

Experimental design

1. Sample size

Describe how sample size was determined.

Sample sizes were calculated with a power analysis before experiments were conducted, except in the case of germfree studies where we were limited by the availability of age and sex matched mice.

415-416 pg 19; 441-442 pg 20; 508-509 pg23; 539-540 pg 24; 571-572 pg 26

2. Data exclusions

Describe any data exclusions.

No data were excluded

3. Replication

Describe whether the experimental findings were reliably reproduced.

Replication attempts were not made.

4. Randomization

Describe how samples/organisms/participants were allocated into experimental groups.

For antibiotic experiments, all dosing was conducted by veterinary technicians who randomly assigned half of the mice to be treated and half to be controls at the beginning of the experiment. (439-441 pg 20)
For diet manipulation experiments, mice were randomly assigned to treatment group by researchers carrying out the experiments. (414-415 pg 19)
For tracer experiments, cages were randomly assigned to treatment by the researcher. (507-508 pg 23)

5. Blinding

Describe whether the investigators were blinded to group allocation during data collection and/or analysis.

Researchers collecting data were blinded to mouse treatment status throughout the antibiotic treatment period. All dosing was conducted by veterinary technicians who were not blinded but did not participate in sample collection or measurement. (439-441 pg 20)
Researchers collecting weight data and fecal samples during diet manipulation experiments were not blinded to treatment, but processing of fecal samples was done by researchers who were blinded to the treatment group until the time of analysis.
Blinding was not performed for stable isotope tracer experiments. (507-508 pg 23)

Note: all studies involving animals and/or human research participants must disclose whether blinding and randomization were used.

6. Statistical parameters

For all figures and tables that use statistical methods, confirm that the following items are present in relevant figure legends (or in the Methods section if additional space is needed).

n/a	Confirmed
☐	☒ The exact sample size (*n*) for each experimental group/condition, given as a discrete number and unit of measurement (animals, litters, cultures, etc.)
☐	☒ A description of how samples were collected, noting whether measurements were taken from distinct samples or whether the same sample was measured repeatedly
☒	☐ A statement indicating how many times each experiment was replicated
☐	☒ The statistical test(s) used and whether they are one- or two-sided (note: only common tests should be described solely by name; more complex techniques should be described in the Methods section)
☐	☒ A description of any assumptions or corrections, such as an adjustment for multiple comparisons
☐	☒ The test results (e.g. *P* values) given as exact values whenever possible and with confidence intervals noted
☐	☒ A clear description of statistics including central tendency (e.g. median, mean) and variation (e.g. standard deviation, interquartile range)
☐	☒ Clearly defined error bars

See the web collection on statistics for biologists for further resources and guidance.

Software

Policy information about availability of computer code

7. Software

Describe the software used to analyze the data in this study.	All data were used with R and standard packages available there within.

For manuscripts utilizing custom algorithms or software that are central to the paper but not yet described in the published literature, software must be made available to editors and reviewers upon request. We strongly encourage code deposition in a community repository (e.g. GitHub). *Nature Methods* guidance for providing algorithms and software for publication provides further information on this topic.

Materials and reagents

Policy information about availability of materials

8. Materials availability

Indicate whether there are restrictions on availability of unique materials or if these materials are only available for distribution by a for-profit company.	n/a

9. Antibodies

Describe the antibodies used and how they were validated for use in the system under study (i.e. assay and species).	n/a

10. Eukaryotic cell lines

a. State the source of each eukaryotic cell line used.	n/a
b. Describe the method of cell line authentication used.	n/a
c. Report whether the cell lines were tested for mycoplasma contamination.	n/a
d. If any of the cell lines used are listed in the database of commonly misidentified cell lines maintained by ICLAC, provide a scientific rationale for their use.	n/a

Animals and human research participants

Policy information about studies involving animals; when reporting animal research, follow the ARRIVE guidelines

11. Description of research animals

Provide details on animals and/or animal-derived materials used in the study.	All animal experiments were performed with adult (8-10 week old) male C57BL/6 mice sourced from Charles River Labs except for germfree mice which were sourced from the Duke Gnotobiotic facility.

Policy information about studies involving human research participants

12. Description of human research participants

Describe the covariate-relevant population characteristics of the human research participants.	Human fecal samples were used in observational analyses. They were sourced from healthy human adults with no use of antibiotics within the past month.